HHS Public Access

Author manuscript

Nat Immunol. Author manuscript; available in PMC 2015 August 01.

Published in final edited form as:

Nat Immunol. 2015 February ; 16(2): 178–187. doi:10.1038/ni.3076.

Regulatory T cells require the phosphatase PTEN to restrain type 1 and follicular helper T-cell responses

Sharad Shrestha[1,2,5], **Kai Yang**[1,5], **Cliff Guy**[1], **Peter Vogel**[3], **Geoffrey Neale**[4], and **Hongbo Chi**[1,2]

[1]Department of Immunology, St. Jude Children's Research Hospital, Memphis, Tennessee 38105, USA

[2]Integrated Biomedical Sciences Program, University of Tennessee Health Science Center, Memphis, Tennessee, 38163, USA

[3]Department of Pathology, St. Jude Children's Research Hospital, Memphis, Tennessee 38105, USA

[4]Hartwell Center for Bioinformatics and Biotechnology, St. Jude Children's Research Hospital, Memphis, Tennessee 38105, USA

Abstract

The interplay between effector and regulatory T (T_{reg}) cells is crucial for adaptive immunity, but how T_{reg} control diverse effector responses is elusive. We found that the phosphatase PTEN links T_{reg} stability to repression of T_H1 and T_{FH} (follicular helper) responses. Depletion of PTEN in T_{reg} resulted in excessive T_{FH} and germinal center responses and spontaneous inflammatory disease. These defects are considerably blocked by deletion of Interferon-γ, indicating coordinated control of T_H1 and T_{FH} responses. Mechanistically, PTEN maintains T_{reg} stability and metabolic balance between glycolysis and mitochondrial fitness. Moreover, PTEN deficiency upregulates mTORC2-Akt activity, and loss of this activity restores PTEN-deficient T_{reg} function. Our studies establish a PTEN-mTORC2 axis that maintains T_{reg} stability and coordinates T_{reg}-mediated control of effector responses.

Introduction

The interplay between immune regulatory mechanisms and effector T cell responses is a crucial determinant of adaptive immunity. Among multiple regulatory systems, thymus-derived regulatory T (T_{reg}) cells marked by the transcription factor Foxp3 play a central role

Correspondence should be addressed to: Hongbo Chi, Department of Immunology, St. Jude Children's Research Hospital, Memphis, TN 38105, USA, Phone: 901-595-6282; Fax: 901-595-5766; hongbo.chi@stjude.org.

[5]These authors contribute equally to this work.

Author contributions: S.S. and K.Y. designed and performed cellular, molecular, and biochemical experiments and contributed to writing the manuscript; C.G. performed imaging assays; P.V. performed hist pathology analysis; GUN. performed Bioinformatics analyses; and H.C designed experiments, wrote the manuscript, and provided overall direction.

Competing financial interests: The authors declare no competing financial interests.

in maintaining self-tolerance and preventing autoimmune disease. Recent genetic studies highlight that T_{reg} cells employ distinct transcriptional programs to control effector T_H1, T_H2 and T_H17 responses[1, 2]. Specifically, T_{reg} cells expressing the transcription factors T-bet, IRF4 and STAT3 orchestrate the control of effector T_H1, T_H2 and T_H17 responses respectively[3-5]. Owing to their potent suppressive activity and functional diversity, the stability of T_{reg} cells is actively maintained by Foxp3-dependent and independent mechanisms[6, 7]. However, under certain inflammatory conditions, T_{reg} cells could lose Foxp3 expression and lineage stability and acquire effector functions[8-11]. Studies also demonstrate the heterogeneity of T_{reg} cells distinguished by the expression of CD25, CCR7 and other molecules[12-14]. Defining the mechanisms involved in the functional diversification and lineage stability of T_{reg} cells is crucial to understanding immune system regulation.

Follicular helper T (T_{FH}) cells are a subset of $CD4^+$T cells specialized in providing help to B cells for the formation of germinal center (GC) reactions and the development of humoral immunity[15]. Excessive T_{FH} responses, however, lead to the development of autoimmune diseases including systemic lupus erythematosus (SLE)[15, 16]. T_{FH} cells are characterized by the preferential expression of the chemokine receptor CXCR5, the co-stimulatory molecule ICOS, the inhibitory molecule PD-1, and the cytokine IL-21. Differentiation of T_{FH} cells requires the interaction with antigen-presenting cells including dendritic cells and B cells, and is further programmed by lineage-specific transcription factors including Bcl6 and Ascl2[15, 17]. Further more, T_{FH} responses are restrained by a specific T_{reg} cell subset, follicular regulatory T cells (T_{FR}), in a Bcl6-dependent manner. T_{FR} cells share phenotypic features with both thymus-derived T_{reg} and T_{FH} cells, as evidenced by the concomitant expression of Foxp3, CTLA4, GITR, Bcl6, ICOS, PD-1 and CXCR5, but are functionally distinct from these conventional populations[18, 19]. The molecular pathways that orchestrate the generation and function of T_{FR} cells and the interplay with other effector cells have remained unclear.

Emerging studies reveal a central role of mechanistic target of rapamycin (mTOR), a signaling pathway that integrates immune and metabolic cues, in T cell-mediated immune responses[20, 21]. mTOR signaling is comprised of two distinct complexes: mTOR complex 1 (mTORC1) and 2 (mTORC2), which have unique contributions to effector T cell responses[22-24], and functional fitness of T_{reg} cells[25]. Because of the potent effects of mTOR signaling on T cell responses, multiple mechanisms are evolved to actively suppress mTOR signaling[20]. For instance, loss of the tumor suppressor Tsc1 aberrantly upregulates mTORC1 activity and disrupts T cell quiescence, homeostasis and functions[26]. T cell-specific deletion of PTEN, an upstream inhibitor of PI3K-Akt signaling, leads to the development of leukemia and autoimmunity[27, 28]. As a pluripotent molecule, PTEN antagonizes PI3K activity and thus inhibits both mTORC1 and mTORC2 activities[20]; PTEN also possesses nuclear functions independent of PI3K-Akt activity[29]. Although PTEN has been implicated in T_{reg} cells from mice and humans[30-32],T_{reg} cells deficient in PTEN show largely normal suppressive activity *in vitro*[33]. Therefore, the functional impacts and molecular pathways of PTEN in T_{reg}-mediated immune homeostasis and function remain to be established.

To investigate the *in vivo* functions and mechanisms of PTEN in T_{reg} cells, we have developed a mouse model to delete PTEN selectively in T_{reg} cells. T_{reg}-specific loss of PTEN is sufficient to induce a systemic lupus-like autoimmune and lymphoproliferative disease. This is associated with excessive T_{FH} and GC B cell responses, as well as exuberant interferon-γ (IFN-γ) production and T_H1 reactions. Deletion of IFN-γ considerably rectifies T_{FH} and autoimmune responses, indicating a crucial role of PTEN in T_{reg} cells at coordinately controlling T_H1 and T_{FH} responses. Mechanistically, PTEN deficiency results in the loss of T_{reg} functional stability and dysregulated transcriptional and metabolic programs, including the balance between glycolytic activity and mitochondrial fitness. Further, PTEN deletion mainly upregulates mTORC2, not mTORC1 activity, in T_{reg} cells. Depletion of Rictor-mTORC2 activity is sufficient to restore the functional abnormalities observed in PTEN-deficient T_{reg} cells. Finally, we present evidence that PTEN is haploinsufficient in T_{reg} cells. Our studies establish a crucial role of the PTEN-mTORC2 axis in mediating T_{reg} cell stability and homeostasis of the immune system, and highlight that their stability is actively maintained to coordinately regulate the magnitude of T_H1 and T_{FH} responses.

Results

T_{reg} deletion of PTEN precipitates an inflammatory disease

To investigate the requirement of PTEN in the homeostasis and functions of $Foxp3^+T_{reg}$ cells, a central regulator of immune tolerance, we crossed mice with *lox*P-flanked *Pten* alleles (*Pten*$^{fl/fl}$) with *Foxp3*$^{YFP\text{-}Cre}$ (*Foxp3*-Cre) mice[34] to delete the *PTEN* conditional alleles specifically in T_{reg} cells but not naive T cells (hereafter *Pten*$^{fl/fl}$*Foxp3*-Cre) (Supplementary Fig. 1a). To examine whether this alters self-tolerance, we measured the amounts of anti-dsDNA and anti-nuclear antigen (ANA) autoantibodies in the serum by ELISA and binding to fixed Hep-2 slides, respectively. As compared with *Foxp3*-Cre mice (designated WT), *Pten*$^{fl/fl}$*Foxp3*-Cre mice contained significantly increased titers of circulating anti-dsDNA and anti-ANA antibodies (Fig. 1a,b), indicative of autoimmune reactions. This was associated with considerably elevated titers of serum IgG2a, IgG2c and IgG2b isotypes in *Pten*$^{fl/fl}$*Foxp3*-Cre mice. In contrast, IgG1 and IgG3 titers were reduced, while IgM and IgA titers were comparable (Supplementary Fig. 1b-d). As systemic autoimmunity is frequently associated with renal pathology, we examined the structural integrity of the kidney. The size and cellularity of the glomeruli were greatly increased in the kidney from *Pten*$^{fl/fl}$*Foxp3*-Cre mice, indicative of glomerulonephritis (Fig. 1c). Moreover, glomeruli of the *Pten*$^{fl/fl}$*Foxp3*-Cre kidney contained prominent IgG deposits (Fig. 1d). Therefore, loss of PTEN in T_{reg} cells results in dysregulation of serum autoantibodies and antibody isotypes and development of renal pathology, indicating a breakdown of immune tolerance in *Pten*$^{fl/fl}$*Foxp3*-Cre mice.

In addition, *Pten*$^{fl/fl}$*Foxp3*-Cre mice spontaneously developed lymphoid hyperplasia, which became prominent when they reached 4-5 months. Specifically, peripheral lymph nodes in *Pten*$^{fl/fl}$*Foxp3*-Cre mice, especially those around the cervical regions, were markedly enlarged. These aged mice also contained a slight increase of the spleen size (Fig. 1e). Moreover, the number and size of lymphoid follicles in Peyer's patches were increased

Pten$^{fl/fl}$*Foxp3*-Cre mice (Fig. 1f). The development of lymphoadenopathy and Peyer's patch abnormality in *Pten*$^{fl/fl}$*Foxp3*-Cremice indicated an ongoing lymphoproliferative disease.

Altered immune homeostasis upon T_{reg}-specific loss of PTEN

The development of the autoimmune and lymphoproliferative disease prompted us to examine whether homeostasis of the immune system was altered in *Pten*$^{fl/fl}$*Foxp3*-Cre mice. In our following analyses, we used mice at a young age, prior to the development of the lymphoproliferative disease. The numbers of $CD4^+$, $CD8^+$, B cells, dendritic cells, and neutrophils were largely comparable between WT and *Pten*$^{fl/fl}$*Foxp3*-Cre mice (Supplementary Fig. 2a-c). However, *Pten*$^{fl/fl}$*Foxp3*-Cre mice contained increased numbers of activated $CD62L^{lo}CD44^{hi}$ effector/memory T cells in the $CD4^+$ and $CD8^+$ compartments (Fig. 2a). Moreover, $CD44^{hi}$ cells from these mice expressed elevated levels of IFN-γ (Fig. 2b). Similarly, expression of CXCR3, a signature chemokine receptor for T_H1 cells, was also increased (Supplementary Fig. 2d). In contrast, IL-17 and IL-4 production was largely normal (Supplementary Fig. 2e). Thus, T cells from *Pten*$^{fl/fl}$*Foxp3*-Cre mice were spontaneously activated *in vivo*, with a propensity to differentiate into the T_H1 phenotype.

Despite severe autoimmune diseases, *Pten*$^{fl/fl}$*Foxp3*-Cre mice had increased percentage and numbers of $Foxp3^+T_{reg}$ cells in the spleen and lymph nodes (Fig. 2c, Supplementary Fig. 2f). To explore the underlying basis for the increased T_{reg} cellularity, we used caspase-3 staining and BrdU incorporation assays to measure T_{reg} apoptosis and proliferation, respectively. T_{reg} cells from WT and *Pten*$^{fl/fl}$*Foxp3*-Cre mice had comparable caspase-3 staining (Fig. 2d), but *Pten*$^{fl/fl}$*Foxp3*-Cre T_{reg} cells had more BrdU incorporation than WT cells (Fig. 2e), indicative of an elevated rate of proliferation. Therefore, PTEN deficiency causes an increased T_{reg} cellularity and proliferation.

Uncontrolled T_{FH} and GC B cells in *Pten*$^{fl/fl}$*Foxp3*-Cre mice

SLE, the prototypical systemic autoimmune disease, is characterized by the heterogeneity of underlying T cell responses. Aside from the roles of the conventional effector (e.g. T_H1 and T_H17) and regulatory responses, recent studies demonstrate a crucial role of T_{FH} cells in the overproduction of pathogenic autoantibodies and tissue damage in SLE[15, 16]. The development of an SLE-like symptom in *Pten*$^{fl/fl}$*Foxp3*-Cre mice prompted us to examine whether the T_{FH} response was altered in these mice. Under steady state, only a small percentage of splenic $CD4^+$T cells was stained positive for the T_{FH} signature molecules CXCR5 and PD-1 in WT mice, but the $CD4^+CXCR5^+PD\text{-}1^+$ population was greatly expanded in the spleen and mesenteric lymph nodes (MLNs) of *Pten*$^{fl/fl}$*Foxp3*-Cre mice (Fig. 3a, Supplementary Fig. 3a). Similar changes were noticed for $CXCR5^+$ cells expressing the T_{FH}-specific co-stimulatory molecule ICOS and transcription factor Bcl6 (Supplementary Fig. 3b,c). The $CD4^+CXCR5^+PD\text{-}1^+$ cells can be further divided into immunostimulatory T_{FH} and immunoregulatory T_{FR} cells, as indicated by the absence or presence of Foxp3 expression, respectively[18, 19]. Both subsets were increased in *Pten*$^{fl/fl}$*Foxp3*-Cre mice (Fig. 3b). Consistent with the increase of $CXCR5^+$ $PD\text{-}1^+$ cells, the spleen and MLNs of *Pten*$^{fl/fl}$*Foxp3*-Cre mice contained 3 fold more GC B cells, denoted by the expression of GC signature markers GL7 and CD95 (Fig. 3c, Supplementary Fig. 3d), even though total B cell numbers were largely unaltered (Supplementary Fig. 2b). Moreover,

immunohistochemistry showed that the spleen and MLNs of *Pten*$^{fl/fl}$*Foxp3*-Cre mice contained considerably more and larger Peanut Agglutinin (PNA)-positive GCs than did their WT counterparts (Fig. 3d,e). These results revealed spontaneous T_{FH} and GC formation in *Pten*$^{fl/fl}$*Foxp3*-Cremice.

We next determined whether PTEN deficiency in T_{reg} cells affects T_{FH} and GC responses after T_{FH}-inducing immunization. After immunization with sheep red blood cells (SRBCs), a strong protein antigen, the formation of T_{FH} cells and GC B cells was greatly enhanced in *Pten*$^{fl/fl}$*Foxp3*-Cre mice compared with WT mice (Fig. 3f,g). We observed a similar finding after challenging WT and *Pten*$^{fl/fl}$*Foxp3*-Cre mice with a T cell-dependent antigen, NP-OVA precipitated in alum together with LPS (Supplementary Fig. 3e,f). We conclude that deletion of PTEN in T_{reg} cells results in enhanced T_{FH} and GC reactions both under steady state and upon immunization.

Coordination of T_H1 and T_{FH} responses by T_{reg} signaling

We next investigated whether the increased T_{FH} response in *Pten*$^{fl/fl}$*Foxp3*-Cre mice was a cell-autonomous defect. To this end, we generated mixed bone marrow (BM) chimeras by reconstituting alymphoid *Rag1*$^{-/-}$ mice with a 1:1 mixture of *Pten*$^{fl/fl}$*Foxp3*-Cre CD45.2$^+$ (donor) and CD45.1$^+$ (spike) BM cells (*Pten*$^{fl/fl}$*Foxp3*-Cre:CD45.1$^+$), and as a control, a mixture of WT and CD45.1 cells (WT:CD45.1$^+$). The frequency of T_{FH} cells was considerably increased in both the donor and spike-derived populations in the *Pten*$^{fl/fl}$*Foxp3*-Cre:CD45.1$^+$ chimeras, as compared with the frequency of T_{FH} cells in the WT:CD45.1$^+$ chimeras (Fig. 4a). Additionally, *Pten*$^{fl/fl}$*Foxp3*-Cre:CD45.1$^+$ chimeras had augmented GC B cells (Fig. 4b). Thus, PTEN deficiency in T_{reg} cells results in a dominantly acting effect on the T_{FH} and GC responses.

We therefore explored whether such defect was associated with dysregulated cytokine production. The T_H1 cytokines such as IFN-γ have been implicated in potentiating T_{FH} responses[35], although opposing evidence also exists[36, 37], suggesting a context-dependent effect. In the *Pten*$^{fl/fl}$*Foxp3*-Cre:CD45.1$^+$ mixed chimeras, IFN-γ production from CD4$^+$ and CD8$^+$T cells was enhanced irrespective of the source of donor cells (Fig. 4c, Supplementary Fig. 4a). To determine the functional effects of the augmented IFN-γ production, we crossed *Pten*$^{fl/fl}$*Foxp3*-Cre mice with *Ifng*$^{-/-}$ mice to generate *Pten*$^{fl/fl}$*Foxp3*-Cre *Ifng*$^{-/-}$ double knockout mice. Deletion of IFN-γ did not exert strong effects on the production of IL-17 and IL-4 from conventional CD4$^+$T cells (Supplementary Fig. 4b). However, IFN-γ deficiency substantially blocked the elevated frequencies of T_{FH} and GC B cells (Fig. 4d,e) and the increased formation of GCs in *Pten*$^{fl/fl}$*Foxp3*-Cre mice (Supplementary Fig. 4c,d). Moreover, the increased production of serum ANA antibody and the deposition of IgG in the kidney glomeruli of *Pten*$^{fl/fl}$*Foxp3*-Cre mice were essentially rectified in *Pten*$^{fl/fl}$*Foxp3*-Cre *Ifng*$^{-/-}$ mice (Fig. 4f,g). Thus, the increased production of IFN-γ in *Pten*$^{fl/fl}$*Foxp3*-Cre mice largely accounts for the exacerbated T_{FH}, GC, and autoimmune responses, thereby highlighting the crucial role of PTEN signaling in T_{reg} cells to coordinate T_H1 and T_{FH} reactions.

PTEN is crucial in maintaining the stability of T_{reg} cells

Despite the crucial role of IFN-γ overproduction in disrupting immune homeostasis in *Pten*$^{fl/fl}$*Foxp3*-Cre mice, deletion of IFN-γ did not affect the phenotype of increased T_{reg} cellularity in these mice (Supplementary Fig. 5a). We therefore explored the direct effects of PTEN deficiency on the homeostasis and functionality of T_{reg} cells. As compared with WT counterparts, T_{reg} cells from *Pten*$^{fl/fl}$*Foxp3*-Cre mice showed higher expression of CD44 and CD69 but lower levels of CD62L, indicating an elevated level of activation (Fig. 5a). We next examined T_{reg}-selective effector molecules. *Pten*$^{fl/fl}$*Foxp3*-CreT_{reg} cells showed increased levels of ICOS and PD-1, and to a lesser extent, GITR, whereas the expression of CTLA4 was largely normal (Fig. 5b). In sharp contrast to the elevated expression of activation markers and effector molecules, expression of CD25, a signature molecule of T_{reg} and activated T cells, was markedly downregulated in *Pten*$^{fl/fl}$*Foxp3*-Cre T_{reg} cells, corresponding to the expansion of the Foxp3^{+}CD25^{-} population (Fig. 5c). As compared with Foxp3^{+}CD25^{+} cells, the Foxp3^{+}CD25^{-} population contained lower levels of Foxp3 expression, as reported previously[12]. Consistent with this observation, Blimp1, a transcription factor implicated in CD25 downregulation in CD8^{+}T cells[38], was upregulated in *Pten*$^{fl/fl}$*Foxp3*-Cre T_{reg} cells (Fig. 5d). These results indicate that PTEN deficiency in T_{reg} cells results in dysregulated expression of multiple T_{reg} activation and phenotypic molecules.

The lineage stability of T_{reg} cells is a matter of considerable interest and debate[6, 8-11, 13], but the signaling mechanisms involved are largely unexplored. To determine whether PTEN deficiency affects the stability of T_{reg} cells, we crossed *Pten*$^{fl/fl}$*Foxp3*-Cre mice with a Cre recombination reporter allele with the ubiquitously expressed Rosa26 locus containing a loxP site–flanked STOP cassette followed by the gene encoding green fluorescent protein (GFP)[25]. In this lineage tracing system, Foxp3^{Cre}-mediated excision of the floxed STOP cassette results in constitutive, heritable expression of GFP, even for those "ex-T_{reg}" cells that have lost Foxp3 expression (the GFP^{+}YFP-Foxp3^{-} population). *Pten*$^{fl/fl}$*Foxp3*-Cre mice contained a striking accumulation of GFP^{+}YFP-Foxp3^{-} population (Fig. 5e), indicating the preferential loss of Foxp3 expression upon PTEN deletion. Additionally, T_{reg} cells from *Pten*$^{fl/fl}$*Foxp3*-Cre mice had increased expression of IFN-γ, whereas IL-17 expression was largely unaltered (Fig. 5f). Moreover, *Pten*$^{fl/fl}$*Foxp3*-Cre T_{reg} cells upregulated signature molecules characteristic of T_H1 and T_{FH} cells, including CXCR3 and T-bet, and CXCR5 and Bcl6, respectively, whereas expression of IRF4 and p-STAT3, which are required for T_{reg}-mediated suppression of T_H2 and T_H17 cells[4, 5], remained unchanged (Supplementary Fig. 5b). Consistent with these observations, *Pten*$^{fl/fl}$*Foxp3*-Cre T_{reg} cells contained an expanded T-bet^{+}CXCR3^{+} population that is important for the regulation of type 1 inflammation (Supplementary Fig. 5c)[3]. Because the development of this T_{reg} subset is dependent upon IFN-γ signaling[3], we examined whether excessive IFN-γ production in *Pten*$^{fl/fl}$*Foxp3*-Cre mice was involved in the dysregulation of T-bet and CXCR3. IFN-γ deficiency had only a partial rescue effect on the expansion of T-bet^{+}CXCR3^{+} population in PTEN-deficient T_{reg} cells (Supplementary Fig. 5c), indicating that the augmented expression of T-bet and CXCR3 upon PTEN deletion is largely cell intrinsic, not simply secondary to the overproduction of IFN-γ. Finally, to directly test the role of PTEN in maintaining T_{reg} stability, we sorted Foxp3^{+}CD25^{+} cells from WT and *Pten*$^{fl/fl}$*Foxp3*-Cre mice and

transferred them into congenic mice (CD45.1$^+$). The expression of Foxp3 and CD25 was downregulated in PTEN-deficient T_{reg} cells in various organs examined, as compared with WT cells (Fig. 5g, Supplementary Fig. 5d). These complementary approaches indicate that PTEN deficiency results in a loss of T_{reg} stability.

Notably, despite the strong effects of IFN-γ at disrupting immune homeostasis (Fig. 4), deletion of IFN-γ in *Pten*$^{fl/fl}$*Foxp3*-Cre mice did not affect the spontaneous development of the Foxp3$^+$CD25$^-$ population (Fig. 5h). Thus, the enhanced IFN-γ expression from *Pten*$^{fl/fl}$*Foxp3*-CreT_{reg} cells is associated with the loss of T_{reg} stability, but is unlikely to be the main driver.

PTEN-dependent transcriptional and metabolic programs

To explore PTEN-dependent molecular mechanisms in T_{reg} cells, we next used microarrays to compare the transcriptional profiles between WT and *Pten*$^{fl/fl}$*Foxp3*-Cre T_{reg} cells. *Pten*$^{fl/fl}$*Foxp3*-Cre T_{reg} cells contained a total of 498 probes (representative of 352 unique genes) with greater than 1.5 fold difference, including 212 upregulated and 286 downregulated probes. Principal component analysis (PCA) showed the clear distinctions between WT and *Pten*$^{fl/fl}$*Foxp3*-Cre samples (Supplementary Fig. 6a). Consistent with the dysregulated stability, loss of PTEN failed to restrain the transcription of genes involved in T_{FH} differentiation, including *Gzmb, Il21, Bcl6, Pdcd1, Il4, Maf* and *Cxcr5*[15, 39] (Fig. 6a). To identify key networks regulated by PTEN, we did gene-set enrichment analysis (GSEA)[40] to compare gene expression profiles of WT and PTEN-deficient T_{reg} cells. Remarkably, the top ten of upregulated gene-sets in *Pten*$^{fl/fl}$*Foxp3*-Cre T_{reg} cells were all associated with cell cycle pathways (Fig. 6b, Supplementary Fig. 6b). To examine PTEN-dependent canonical pathways in T_{reg} cells, we next performed the ingenuity pathway analysis (IPA) system by interrogating the differentially expressed genes at the 1.5 fold cut-offs. As shown in Fig. 6c, PTEN deficiency affected multiple canonical pathways implicated in autoimmune diseases, helper T cell differentiation, and immune signaling mediated by transcription factors, co-stimulatory molecules and cytokines. Gene ontology (GO) analysis of these differentially regulated genes also showed that PTEN-deficient T_{reg} cells significantly upregulated groups of genes involved in autoimmune diseases, such as autoimmune thyroid disease and SLE, as well as in cell cycle regulation (data not shown). The transcriptome analysis therefore highlights an important role of PTEN in the regulation of immune response and cell cycle pathways.

Cellular metabolic programs, especially glycolysis and mitochondrial oxidative phosphorylation, play an important role in shaping T_{reg} generation and function[41, 42], although the molecular mechanisms are unknown. As compared with WT T_{reg} cells, *Pten*$^{fl/fl}$*Foxp3*-Cre T_{reg} cells more strongly upregulated glycolysis after TCR/CD28 stimulation (Fig. 6d). We next examined whether PTEN deficiency affects mitochondrial fitness by measuring multiple parameters associated with mitochondria homeostasis and functions. *Pten*$^{fl/fl}$*Foxp3*-Cre T_{reg} cells showed considerable reduction of reactive oxidative species (ROS), mitochondrial mass, and mitochondrial membrane potential, indicative of impaired mitochondrial fitness (Fig. 6e). Notably, the reduction of these parameters was more prominent in PTEN-deficient Foxp3$^+$CD25$^-$ T_{reg} cells than Foxp3$^+$CD25$^+$ cells (Fig.

6e), indicating that impaired mitochondrial function is associated with T_{reg} instability. Moreover, the $Foxp3^{+}CD25^{-}$ T_{reg} subset showed a modestly stronger phenotype of BrdU incorporation than $Foxp3^{+}CD25^{+}$ cells (Fig. 6f). Altogether, these data establish that PTEN signaling links immune response gene expression, cell cycle progression, and metabolic balance between glycolytic activity and mitochondrial fitness in T_{reg} cells.

PTEN signals via mTORC2 inhibition in T_{reg} cells

We determined PTEN-dependent biochemical mechanisms in T_{reg} cells by examining mTORC1 and mTORC2 activities, as both are under the control of PTEN in multiple cell types[20]. In response to short-term anti-CD3-CD28 stimulation (5-15 min), *Pten*$^{fl/fl}$*Foxp3*-Cre T_{reg} cells exhibited slightly elevated phosphorylation of the mTORC1 target S6, as compared with WT T_{reg} cells (Fig. 7a, Supplementary Fig. 7a). In contrast, *Pten*$^{fl/fl}$*Foxp3*-Cre T_{reg} cells exhibited much stronger activation of mTORC2 signaling than WT cells, as indicated by the enhanced phosphorylation of Akt at Ser473 and of the Akt downstream target Foxo1 (Fig. 7a). We next determined the effects of stimulating T_{reg} cells with anti-CD3-CD28 for a longer time (20 h), in the presence or absence of IL-2. Both WT and *Pten*$^{fl/fl}$*Foxp3*-Cre T_{reg} cells responded to these stimuli with robust phosphorylation of S6 and 4E-BP1, indicative of comparable activation of the mTORC1 pathway under these conditions (Fig. 7b, Supplementary Fig. 7b). In contrast, *Pten*$^{fl/fl}$*Foxp3*-Cre T_{reg} cells exhibited much stronger activation of mTORC2 signaling than WT cells (Fig. 7b). Therefore, loss of PTEN results in preferential activation of mTORC2 signaling in T_{reg} cells.

To determine the contribution of mTORC2 activity to *Pten*$^{fl/fl}$*Foxp3*-Cre phenotypes, we crossed *Pten*$^{fl/fl}$*Foxp3*-Cre mice with those lacking Rictor that abrogated mTORC2 activity (*Pten*$^{fl/fl}$*Foxp3*-Cre)[25] to generate *Pten*$^{fl/fl}$*Rictor*$^{fl/fl}$*Foxp3*-Cre mice. Compared with *Pten*$^{fl/fl}$*Foxp3*-Cre T_{reg} cells with increased cellularity but diminished CD25 expression, T_{reg} cells in *Pten*$^{fl/fl}$*Rictor*$^{fl/fl}$*Foxp3*-Cre mice exhibited normal abundance and CD25 expression (Fig. 7c). Other T_{reg} markers analyzed were also considerably rescued by the deletion of Rictor from *Pten*$^{fl/fl}$*Foxp3*-Cre T_{reg} cells (Supplementary Fig. 7c). Additionally, T cells in *Pten*$^{fl/fl}$*Rictor*$^{fl/fl}$*Foxp3*-Cre mice exhibited largely normal distribution of naïve and effector/memory phenotypes (Supplementary Fig. 7d). Also, the spontaneous development of T_{FH} and T_H1 cells and GC B cells observed in *Pten*$^{fl/fl}$*Foxp3*-Cre mice was blocked by Rictor deletion (Fig. 7d, Supplementary Fig. 7e). Moreover, unlike *Pten*$^{fl/fl}$*Foxp3*-Cre mice, *Pten*$^{fl/fl}$*Rictor*$^{fl/fl}$*Foxp3*-Cre mice did not contain IgG deposits in the kidney glomeruli (Fig. 7e), and exhibited normal GC numbers in the spleen and MLNs (Supplementary Fig. 7f,g). Therefore, despite the plethora of pathways identified to mediate PTEN functions in various cells[20], PTEN acts in an mTORC2-dependent manner in T_{reg} cells to impinge upon immune homeostasis and tolerance.

PTEN is haploinsufficient in T_{reg} cells

Given the potent effects of PTEN signaling in T_{reg} cells, we asked whether partial loss of PTEN function in T_{reg} cells is physiologically relevant, by analyzing *Pten*$^{fl/+}$*Foxp3*-Cre mice. As expected, *Pten*$^{fl/+}$*Foxp3*-Cre T_{reg} cells, but not other T cell subsets, had partial reduction of PTEN expression at both the mRNA and protein levels (Supplementary Fig.

8a,b). Remarkably, heterozygous loss of PTEN resulted in the expansion of T_{reg} cells, associated with considerable downregulation of CD25 expression (Fig. 8a). *Pten*$^{fl/+}$*Foxp3*-Cre mice also contained a striking accumulation of GFP^{+}YFP-Foxp3^{-} population in the lineage tracing system (Fig. 8b). Moreover, these mice contained increased CXCR5^{+}PD-1^{+} T_{FH} cells and GL7^{+}CD95^{+} GC B cells (Fig. 8c), and more abundance of GCs in the spleen (Supplementary Fig. 8c). These findings prompted us to examine whether heterozygous loss of PTEN in T_{reg} cells caused autoimmunity and lymphoid hyperplasia as observed in *Pten*$^{fl/fl}$*Foxp3*-Cre mice. *Pten*$^{fl/+}$*Foxp3*-Cre mice displayed significantly elevated titers of circulating anti-ANA antibodies (Fig. 8d) and augmented IgG deposits in the kidney glomeruli (Fig. 8e), indicative of systemic autoimmunity. Furthermore, *Pten*$^{fl/+}$*Foxp3*-Cre mice spontaneously developed lymphoadenopathy (Supplementary Fig. 8d). These results demonstrate that PTEN is haploin sufficient in T_{reg} cells.

Discussion

Extensive progress has been made on the transcriptional and molecular pathways underlying effector T cell diversity and plasticity. In contrast, how these distinct effector T cell responses are controlled by extrinsic mechanisms is poorly understood. Moreover, despite the emerging evidence for the adoption of T_H-specific transcription factors by T_{reg} cells to suppress the corresponding effector responses[3-5], we have little understanding about the signaling mechanisms that program these suppressive activities. Here we, together with Huynh *et al.* (companion manuscript), identify PTEN as a crucial molecular pathway in T_{reg} cells that coordinately regulates T_{FH} and T_H1 responses (Supplementary Fig. 8e). In particular, loss of PTEN in T_{reg} cells results in exacerbated T_{FH} and GC responses and disrupted immune tolerance and homeostasis. Ablation of IFN-γ function reveals the hierarchy between T_{reg}-mediated control of T_H1 and T_{FH} responses, with the production of the T_H1 signature cytokine IFN-γ a prerequisite for the potentiation of T_{FH} responses in *Pten*$^{fl/fl}$*Foxp3*-Cre mice. Further more, the repression of T_H1 and T_{FH} responses is associated with the active maintenance of T_{reg} cell stability enforced by PTEN signaling. At the molecular levels, PTEN controls the transcriptional program and metabolic balance in T_{reg} cells, and it mainly signals via inhibition of mTORC2 activity. Our studies therefore establish that the PTEN-mTORC2 axis acts as a central pathway to orchestrate T_{reg} cell stability and restrict T_H1 and T_{FH} responses.

The lineage stability of T_{reg} cells remains contentious[6, 8-13] but is an issue of utmost importance, as it directly impinges upon T_{reg}-mediated control of health and disease and therapeutic strategies[2]. Using lineage tracing and adoptive transfer systems, we show that PTEN-deficient T_{reg} cells are more prone to lose Foxp3 expression *in vivo*. Moreover, PTEN deficiency results in apparently hyper-activated T_{reg} cells, as evidenced by increased cycling, upregulation of activation and phenotypic markers, and aberrant induction of T_H1 and T_{FH} signature molecules. Consistent with this, PTEN deletion results in loss of CD25 expression, which is normally downregulated in T_{reg} cells after *in vivo* activation and proliferation[43]. While representing only a minor proportion of Foxp3^{+} T_{reg} cells under steady state, the Foxp3^{+}CD25^{-} population likely makes an important contribution, via conversion or selection, to the generation of ex-T_{reg} cells under inflammatory or lymphopenic environment. Therefore, our studies highlight that the stability of T_{reg} cells

under steady state requires active enforcement by PTEN, which functions, at least in part, by preventing overt T_{reg} activation and CD25 downregulation.

Generation of T_{FH} cells requires unique transcriptional programs and is antagonized by T_{FR} cells[18, 19]. However, T_{FR} cells can also promote antigen-specific high-affinity B cell responses[19] and influenza-specific GC reactions[44]. Extensive crosstalk also exists between the differentiation of T_{FH} cells and other effector lineages[15]. Here we show that PTEN signaling in T_{reg} cells is crucial in the repression of T_{FH} responses, which is further linked to T_{reg} stability and T_{reg}-mediated control of T_H1 responses. Strikingly, loss of PTEN in T_{reg} cells results in spontaneous T_{FH} differentiation and GC formation, and the development of SLE-like autoimmune symptoms. Associated with these immune defects is the dysregulated expression of multiple molecules involved in T_{FH} and T_{FR} responses, including IL-4, IL-21, Bcl6, Blimp1 and Granzyme B, which likely underlies the loss of proper T_{FR} functions in PTEN-deficient T_{reg} cells. Moreover, the uncontrolled T_{FH} responses in *Pten*$^{fl/fl}$*Foxp3*-Cre mice are dependent upon the T_H1 signature cytokine IFN-γ. Notably, the relationship between T_H1 and T_{FH} cells is complex and remains controversial. For instance, whereas IFN-γ is essential in driving T_{FH} cells in the *Roquin*$^{san/san}$ autoimmunity model[35], it is dispensable for the differentiation of T_{FH} cells induced by viral infection[37]. Further, T-bet induction dampens rather than enhances the T_{FH} differentiation program[36]. Our studies demonstrate that T_{FH} and T_H1 responses are coordinately regulated by T_{reg} cells, with the IFN-γ production required for T_{FH} and GC reactions. However, we cannot conclude the direct contribution of the exacerbated T_H1 response, independent of T_{FH} cells, to the autoimmune and lymphoproliferative phenotypes.

As one of the most frequently mutated tumor suppressor genes, PTEN acts in murine T cells to prevent development of leukemia and autoimmunity[27]. More recent studies unveil that these two effects can be dissociated as they are derived from abnormalities in the thymus and periphery, respectively[28]. PTEN is also implicated in the regulation of effector T cell responses. Deletion of PTEN in activated T cells enhances effector responses but does not lead to autoimmunity or cancer[45]. miRNAs targeting PTEN expression are also implicated in shaping T_{FH} responses[46]. We found that deletion of PTEN in T_{reg} cells leads to the exacerbated effector T cell responses and loss of immune tolerance and tissue homeostasis. PTEN-deficient T_{reg} cells dominate over WT cells in mediating T_{FH} and GC responses, which are mediated, at least in part, by dysregulated IFN-γ expression. Moreover, PTEN functions in a haploin sufficient manner in T_{reg} cells. These results together establish PTEN signaling in T_{reg} cells as a unique regulator of immune homeostasis and function.

How does PTEN function in T_{reg} cells at the molecular levels? Our microarray, metabolic and immunological assays reveal the important role of PTEN in linking cell cycle and metabolic machineries and expression of immune effector genes in T_{reg} cells. Given the opposing effects of glycolytic and mitochondrial metabolism on T_{reg} cells[41, 42], the disrupted balance between these activities in PTEN-deficient T_{reg} cells is likely an important contributor to the phenotypic alteration, a notion that requires additional investigation. Of note, despite the metabolic functions of PTEN identified in non-immune cells, the underlying mechanisms are highly complex and poorly understood[47]. Here we establish the PTEN-mTORC2 axis as a central determinant of T_{reg} stability and T_{reg}-mediated control of

effector responses, although the involvement of mTORC2-independent pathways cannot be excluded[48]. Mechanistically, this signaling pathway likely orchestrates both the metabolic and transcriptional programs, such as those mediated by Foxo1 and Blimp1[7, 38], in impinging upon T_{reg} stability and functions. We note that loss of T_{reg} stability also results from T_{reg}-specific deletion of neuropilin-1 and Foxo1[7, 32], and future work is required to explore the crosstalk between these molecular pathways in T_{reg} cells.

In summary, our study has unveiled the interplay between the PTEN-mTORC2 signaling axis and the transcriptional and metabolic regulation in T_{reg} cells as a new mechanism for enforcing T_{reg} stability and T_{reg}-mediated repression of T_H1 and T_{FH} responses. Given the potent effects of selective PTEN deficiency in T_{reg} cells on immune tolerance and tissue homeostasis, even under steady state conditions or upon a partial loss of function, the identification of this signaling axis provides a new target for therapeutic intervention of systemic autoimmune and lymphoproliferative diseases.

Methods

Mice

Pten$^{fl/fl}$, CD45.1^{+}, *Rag1*$^{-/-}$, *Ifng*$^{-/-}$ and Rosa26^{GFP} (a loxP-site-flanked STOP cassette followed by the GFP-encoding sequence was inserted into the Rosa26 locus) mice were purchased from the Jackson Laboratory. *Rictor*$^{-/-}$ mice have been described previously[25]. *Foxp3*$^{YFP\text{-}Cre}$ mice were a gift from A. Rudensky[34]. *Pten*$^{fl/fl}$*Foxp3*-Cre mice were used at 10-12 weeks old unless otherwise noted, with the age and gender-matched WT mice containing the *Foxp3*^{cre} allele as controls. BM chimeras were generated by transferring 7 × 10^6 T-cell-depleted BM cells into sub-lethally irradiated (5 Gy) *Rag1*$^{-/-}$ mice, followed by reconstitution for at least 2.5 months. All mice were kept in a specific pathogen-free facility in the Animal Resource Center at St. Jude Children's Research Hospital. Animal protocols were approved by the Institutional Animal Care and Use Committee of St. Jude Children's Research Hospital.

Flow cytometry

For analysis of surface markers, cells were stained in PBS containing 2% (wt/vol) BSA, with anti-CD4 (RM4-5), anti-CD8α (53-6.7), anti-TCRβ (H57-597), anti-CD69 (H1.2F3), anti-CD25 (PC61.5), anti-CD44 (1M7), anti-CD62L (MEL-14), anti-CD45.1 (A20), anti-CD45.2 (104), anti-PD-1 (J43), anti-GL7 (GL-7), anti-CD95 (15A7), anti-ICOS (C398.4A), anti-GITR (DTA-1), anti-CD19 (1D3), anti-CXCR3 (CXCR3-173), anti-MHCII (M5/114.15.2), anti-CD11b (M1/70), anti-CD11c (N418), anti-Ly6G (RB6-8C5; all from eBioscience). CXCR5 was stained with biotinylated anti-CXCR5 (clone 2G8) and streptavid in-conjugated PE (both from BD Biosciences). Intracellular Foxp3 (FJK-16s), T-bet (4B10), IRF4 (3E4), IFN-γ (XMG1.2), IL-4 (11B11), IL-17 (17B7; all from eBioscience), CTLA4 (UC10-4B9; BioLegend), p-STAT3 (4/P-STAT3), PTEN (A2B1), Bcl6 (K112-91; all from BD Biosciences) were analyzed by flow cytometry according to the manufacturer's instructions. Blimp1 (3H2-E8) was purchased from Thermo Scientific. For intracellular cytokine staining, T cells were stimulated for 4 h with PMA plus ionomycin in the presence of monensin before being stained according to the manufacturer's instructions (eBioscience).

BrdU and caspase-3 staining was performed as per the manufacturer's instruction (BD Biosciences). For staining mitochondria, lymphocytes were incubated for 30 min at 37°C with 10 nM Mito Tracker Deep Red (Life Technologies) or 20 nM TMRM (tetramethylrhodamine, methyl ester; ImmunoChemistry Technologies) after staining surface markers. ROS were measured by incubation with 5 μMMito SOX™ Red (Life Technologies) after staining surface markers. Flow cytometry data were acquired on LSRII or LSR Fortessa (BD Biosciences) and analyzed using Flowjo software (Tree Star).

Imaging and immunohistochemistry

For cryosections, kidneys and MLNs were freshly frozen in OCT embedding medium. Ten μm thick cryosections were fixed with cold acetone for 5 min prior to rehydration in TBS. Non-specific binding was blocked by incubation in TBS containing 2% BSA and 5% normal donkey serum for 30 min prior to incubation with primary antibodies (2 μg/ml) overnight at 4°C. Slides were washed for 15 min in TBS prior to incubation with AF568-conjugated goat anti-mouse antibody (1 μg/ml; Life Technologies), AF568-conjugated donkey anti-goat antibody (1 μg/ml; Life Technologies), Cy5-conjugated donkey anti-goat antibody (1 μg/ml; Jackson ImmunoResearch), or AF488-conjugated streptavid in (1 μg/ml; Life Technologies) for 1 h at room temperature. Slides were washed for 15 min in TBS prior to mounting in Vectashield hard set with DAPI (Vector Laboratories). Fluorescent images were acquired using a Zeiss Axiovert 200M and 20X EC Plan-NeoFluar objective, detected using a Cascade II EMCCD camera (Photometrics) and analyzed using Slidebook software (3i Intelligent Imaging Innovations). Large image composites were acquired with a Nikon Ti-E inverted microscope with 20X CFI Plan Apochromat Lambda objective and iXon DU897 EMCCD camera, using NIS-Elements software. Visualization of ANA antibodies was performed by staining fixed Hep-2 slides (MBL). Specifically, serum samples were applied to the slide and incubated for 2 h at room temperature followed by 15 min washing in TBS. Bound murine antibodies were detected using AF568-conjugated goat anti-mouse antibody (1 μg/ml; Life Technologies) for 1 h at room temperature, while AF488-conjugated phalloidin (Life Technologies) was utilized to visualize f-Actin and nuclei were detected using DAPI. CD3 (sc-1127 (M-20)) antibody was purchased from Santa Cruz, Biotinylated Peanut Agglutinin (PNA) from Vector Laboratories (B-1075), and IgD (558597) from BD Biosciences.

For paraffin sections, spleen, kidney and Peyer's patches were fixed by immersion in 10% (vol/vol) neutral buffered formalin solution. Fixed tissues were embedded in paraffin, sectioned and stained with hematoxylin and eosin, and the clinical signs of autoimmune diseases were analyzed by an experienced pathologist (P. Vogel).

Immunization

For experiments involving antigen-induced T_{FH} and GC B cell response, antigen for immunization was prepared by mixing NP_{14}-OVA (14 molecules of NP linked to OVA; Biosearch Technologies), 10% $KAl(SO_4)_2$ dissolved in PBS at a ratio of 1:1, in the presence of LPS (*Escherichia coli* strain 055:B5; Sigma) and at pH 7. NP-OVA (100 μg) and LPS (10 μg) precipitated in alum was injected intraperitoneally, as described[46]. Alternatively, a fresh

preparation of PBS-washed (1×10^9) SRBCs from Colorado Serum Company (31112) was injected intravenously to induce a robust splenic GC response.

Serum antibodies

Autoantibodies (dsDNA) and immunoglobulin subclasses were measured with kits from Alpha Diagnostic International (5110) and Millipore (MGAMMAG-300K), respectively.

Cell purification and adoptive transfer

Lymphocytes were isolated from lymphoid organs (spleen and peripheral lymph nodes that included inguinal, auxiliary and cervical lymph nodes) and naïve and T_{reg} cells were sorted on a MoFlow (Beckman-Coulter) or Reflection (i-Cyt). For adoptive transfer, $CD4^+CD25^+$Foxp3-YFP^+ cells from WT and *Pten*$^{fl/fl}$*Foxp3*-Cre mice ($CD45.2^+$) were transferred to the congenically marked ($CD45.1^+$) recipients. Seven days after the transfer, mice were euthanized for the analysis of Foxp3 and CD25 expression.

RNA and immunoblot analysis

Real-time PCR analysis was performed with primers and probe sets from Applied Biosystems, as described[49]. Immunoblots were performed as described previously[50], using the following antibodies: p-S6 (2F9), p-4E-BP1 (236B4), p-Foxo1 (9461), Akt phosphorylated at Ser473 (D9E), PTEN (138D6; all from Cell Signaling Technology), and β-actin (AC-15; Sigma).

Glycolysis assay

T_{reg} cells were stimulated with plate-bound anti-CD3-CD28 for 6 h, and glycolytic flux was measured by detritiation of [3-^{3}H]-glucose, as previously described[42].

Gene expression profiling and gene-set enrichment analysis

RNA samples from freshly isolated T_{reg} cells from WT and *Pten*$^{fl/fl}$*Foxp3*-Cremice were analyzed with the Affymetrix HT MG-430 PM Gene Titan peg array, and expression signals were summarized with the robust multi-array average algorithm (Affymetrix Expression Console v1.1). Lists of differentially expressed genes by 1.5 fold or more were analyzed for functional enrichment using the Ingenuity Pathways (www.ingenuity.com). Gene-set enrichment analysis within canonical pathways was performed as described[40]. The microarray data has been deposited into the GEO series database (GSE63625).

Statistical analysis

P values were calculated with Student's t-test (GraphPad Prism). P values of less than 0.05 were considered significant. All error bars represent the s.e.m.

Supplementary Material

Refer to Web version on PubMed Central for supplementary material.

Acknowledgments

The authors acknowledge J. Wei, D. Bastardo Blanco and S. Brown for help with immunological assays, and C. Cloer and B. Rhode animal colony management, A. Rudensky for *Foxp3*$^{YFP\text{-}Cre}$ mice, and St. Jude Immunology FACS core facility for cell sorting. This work was supported by NIH AI105887, AI101407, CA176624 and NS064599, American Cancer Society, and Crohn's & Colitis Foundation of America (to H.C.), and by a postdoctoral fellowship from the Arthritis Foundation (to K.Y.).

References

1. Josefowicz SZ, Lu LF, Rudensky AY. Regulatory T cells: mechanisms of differentiation and function. Annu Rev Immunol. 2012; 30:531–564. [PubMed: 22224781]
2. Sakaguchi S, Vignali DA, Rudensky AY, Niec RE, Waldmann H. The plasticity and stability of regulatory T cells. Nat Rev Immunol. 2013; 13:461–467. [PubMed: 23681097]
3. Koch MA, et al. The transcription factor T-bet controls regulatory T cell homeostasis and function during type 1 inflammation. Nat Immunol. 2009; 10:595–602. [PubMed: 19412181]
4. Zheng Y, et al. Regulatory T-cell suppressor program co-opts transcription factor IRF4 to control T(H)2 responses. Nature. 2009; 458:351–356. [PubMed: 19182775]
5. Chaudhry A, et al. CD4+ Regulatory T Cells Control TH17 Responses in a Stat3-Dependent Manner. Science. 2009
6. Rubtsov YP, et al. Stability of the regulatory T cell lineage in vivo. Science. 2010; 329:1667–1671. [PubMed: 20929851]
7. Ouyang W, et al. Novel Foxo1-dependent transcriptional programs control T(reg) cell function. Nature. 2012; 491:554–559. [PubMed: 23135404]
8. Zhou X, et al. Instability of the transcription factor Foxp3 leads to the generation of pathogenic memory T cells in vivo. Nat Immunol. 2009; 10:1000–1007. [PubMed: 19633673]
9. Tsuji M, et al. Preferential generation of follicular B helper T cells from Foxp3+ T cells in gut Peyer's patches. Science. 2009; 323:1488–1492. [PubMed: 19286559]
10. Bailey-Bucktrout SLE, et al. Self-antigen-driven activation induces instability of regulatory T cells during an inflammatory autoimmune response. Immunity. 2013; 39:949–962. [PubMed: 24238343]
11. Comatose N, et al. Pathogenic conversion of Foxp3+ T cells into TH17 cells in autoimmune arthritis. Nat Med. 2014; 20:62–68. [PubMed: 24362934]
12. Comatose N, et al. Heterogeneity of natural Foxp3+ T cells: a committed regulatory T-cell lineage and an uncommitted minor population retaining plasticity. Proc Natl Acad Sci U S A. 2009; 106:1903–1908. [PubMed: 19174509]
13. Miaow T, et al. Plasticity of Foxp3(+)T cells reflects promiscuous Foxp3 expression in conventional T cells but not reprogramming of regulatory T cells. Immunity. 2012; 36:262–275. [PubMed: 22326580]
14. Miguel KS, et al. CCR7 provides localized access to IL-2 and defines home statically distinct regulatory T cell subsets. J Exp Med. 2014; 211:121–136. [PubMed: 24378538]
15. Corty S. Follicular helper CD4 T cells (FH). Annu Rev Immunol. 2011; 29:621–663. [PubMed: 21314428]
16. Linter man MA, et al. Follicular helper T cells are required for systemic autoimmunity. J Exp Med. 2009; 206:561–576. [PubMed: 19221396]
17. Liu X, et al. Transcription factor achaete-scute homologue 2 initiates follicular T-helper-cell development. Nature. 2014; 507:513–518. [PubMed: 24463518]
18. Chang Y, et al. Follicular regulatory T cells expressing Foxp3 and Bcl-6 suppress germinal center reactions. Nat Med. 2011; 17:983–988. [PubMed: 21785430]
19. Linter man MA, et al. Foxp3+ follicular regulatory T cells control the germinal center response. Nat Med. 2011; 17:975–982. [PubMed: 21785433]
20. Chi H. Regulation and function of mTOR signalling in T cell fate decisions. Nat Rev Immunol. 2012; 12:325–338. [PubMed: 22517423]

21. Powell JD, Pol lizzie KN, Headlamp EB, Horton MR. Regulation of immune responses by mTOR. Annu Rev Immunol. 2012; 30:39–68. [PubMed: 22136167]
22. Lee K, et al. Mammalian target of rapamycin protein complex 2 regulates differentiation of Th1 and Th2 cell subsets via distinct signaling pathways. Immunity. 2010; 32:743–753. [PubMed: 20620941]
23. Del gaffe GM, et al. The kins mTOR regulates the differentiation of helper T cells through the selective activation of signaling by mTORC1 and mTORC2. Nat Immunol. 2011; 12:295–303. [PubMed: 21358638]
24. Yang K, et al. T Cell Exit from Quiescence and Differentiation into Th2 Cells Depend on Raptor-mTORC1-Mediated Metabolic Reprogramming. Immunity. 2013; 39:1043–1056. [PubMed: 24315998]
25. Zing H, et al. mTORC1 couples immune signals and metabolic programming to establish T(reg)-cell function. Nature. 2013; 499:485–490. [PubMed: 23812589]
26. Yang K, Neale G, Green DR, He W, Chi H. The tumor suppressor Tsc1 enforces quiescence of naive T cells to promote immune homeostasis and function. Nat Immunol. 2011; 12:888–897. [PubMed: 21765414]
27. Suki A, et al. T cell-specific loss of Pten leads to defects in central and peripheral tolerance. Immunity. 2001; 14:523–534. [PubMed: 11371355]
28. Liu X, et al. Distinct roles for PTEN in prevention of T cell lymphoma and autoimmunity in mice. J Cling Invest. 2010; 120:2497–2507.
29. Song MS, et al. Nuclear PTEN regulates the APC-CDH1 tumor-suppressive complex in a phosphatase-independent manner. Cell. 2011; 144:187–199. [PubMed: 21241890]
30. Ben singer SJ, et al. Distinct IL-2 receptor signaling pattern in CD4+CD25+ regulatory T cells. J Immunol. 2004; 172:5287–5296. [PubMed: 15100267]
31. Zanin-Zhorov A, et al. Scaffold protein Disc large homology 1 is required for T-cell receptor-induced activation of regulatory T-cell function. Proc Natl Acad Sci U S A. 2012; 109:1625–1630. [PubMed: 22307621]
32. Del gaffe GM, et al. Stability and function of regulatory T cells is maintained by a neuropilin-1-semaphorin-4a axis. Nature. 2013; 501:252–256. [PubMed: 23913274]
33. Walsh PT, et al. PTEN inhibits IL-2 receptor-mediated expansion of CD4+ CD25+ Trigs. J Cling Invest. 2006; 116:2521–2531.
34. Rubtsov YP, et al. Regulatory T cell-derived interleukin-10 limits inflammation at environmental interfaces. Immunity. 2008; 28:546–558. [PubMed: 18387831]
35. Lee SK, et al. Interferon-gamma excess leads to pathogenic accumulation of follicular helper T cells and germinal centers. Immunity. 2012; 37:880–892. [PubMed: 23159227]
36. Nakayamada S, et al. Early Th1 cell differentiation is marked by a FH cell-like transition. Immunity. 2011; 35:919–931. [PubMed: 22195747]
37. Ray JP, et al. Transcription factor STAT3 and type I interferon's are co repressive insulators for differentiation of follicular helper and T helper 1 cells. Immunity. 2014; 40:367–377. [PubMed: 24631156]
38. Shin HM, et al. Epigenetic modifications induced by Blimp-1 Regulate CD8 (+) T cell memory progression during acute virus infection. Immunity. 2013; 39:661–675. [PubMed: 24120360]
39. Wang H, et al. The transcription factor Foxp1 is a critical negative regulator of the differentiation of follicular helper T cells. Nat Immunol. 2014; 15:667–675. [PubMed: 24859450]
40. Sub romanian A, et al. Gene set enrichment analysis: a knowledge-based approach for interpreting genome-wide expression profiles. Proc Natl Acad Sci U S A. 2005; 102:15545–15550. [PubMed: 16199517]
41. Michael RD, et al. Cutting edge: Distinct glycolytic and lipid oxidative metabolic programs are essential for effector and regulatory CD4+ T cell subsets. J Immunol. 2011; 186:3299–3303. [PubMed: 21317389]
42. Chi LS, et al. HIF1a-dependent glycolytic pathway orchestrates a metabolic checkpoint for the differentiation of TH17 and Trig cells. J Exp Med. 2011; 208:1367–1376. [PubMed: 21708926]

43. Gavin MA, Clarke SR, Negro E, Gall egos A, Rudensky A. Homeostasis and energy of CD4(+)CD25(+) suppressor T cells in vivo. Nat Immunol. 2002; 3:33–41. [PubMed: 11740498]
44. Leon B, Bradley J, Land FE, Randall TD, Ballesteros-Tato A. FoxP3+ regulatory T cells promote influenza-specific FH responses by controlling IL-2 availability. Nat Common. 2014; 5:3495.
45. Sound DR, et al. Pten loss in CD4 T cells enhances their helper function but does not lead to autoimmunity or lymphoma. J Immunol. 2012; 188:5935–5943. [PubMed: 22611241]
46. Lang AG, et al. MicroRNAs of the miR-17 approximately 92 family are critical regulators of T(FH) differentiation. Nat Immunol. 2013; 14:849–857. [PubMed: 23812097]
47. Garcia-Cao I, et al. Systemic elevation of PTEN induces a tumor-suppressive metabolic state. Cell. 2012; 149:49–62. [PubMed: 22401813]
48. Wei J, Yang K, Chi H. Cutting Edge: Discrete Functions of mTOR Signaling in Invariant NET Cell Development and NKT17 Fate Decision. J Immunol. 2014; 193:4297–4301. [PubMed: 25261481]
49. Liu G, et al. The receptor S1P1 overrides regulatory T cell-mediated immune suppression through Akt-mTOR. Nat Immunol. 2009; 10:769–777. [PubMed: 19483717]
50. Liu G, Yang K, Burns S, Shrestha S, Chi H. The S1P(1)-mTOR axis directs the reciprocal differentiation of T(H)1 and T(reg) cells. Nat Immunol. 2010; 11:1047–1056. [PubMed: 20852647]

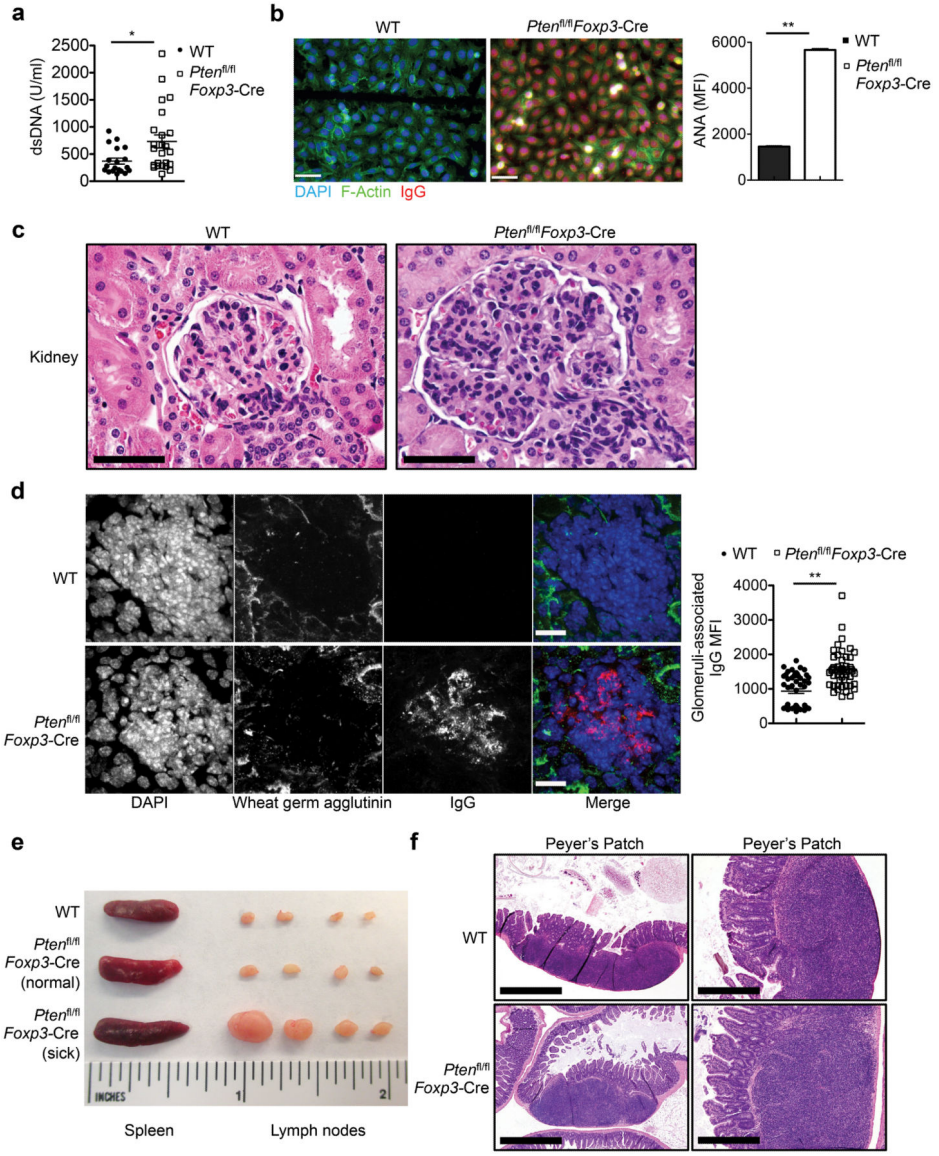

Figure 1. *Pten*$^{fl/fl}$*Foxp3*-Cremice develop age-related autoimmune and lymphoproliferative disease

(**a**) Quantification of dsDNA-specific IgG in the serum of *Pten*$^{+/+}$*Foxp3*-Cre (WT) and *Pten*$^{fl/fl}$*Foxp3*-Cre mice (2-6 months old). (**b**) Representative images (scale 60 μm) and quantification of fluorescent intensity (right) of serum ANA IgG autoantibodies detected with fixed Hep-2 slides. (**c**) Histology images of kidney glomeruli sections stained with H&E (magnification: ×60; scale 50 μm). (**d**) Immune fluorescence images of kidney glomeruli sections showing IgG deposits (scale 40 μm). (**e**) Images of spleen and peripheral lymph nodes from WT (upper, ∼5 months old), *Pten*$^{fl/fl}$*Foxp3*-Cre mice prior to the development of lymphoproliferative disease (middle, ∼2.5 months old), and *Pten*$^{fl/fl}$*Foxp3*-Cre mice with lymphoproliferative disease (lower, ∼5 months old). (**f**) H&E staining of Peyer's patches in the intestine of WT and *Pten*$^{fl/fl}$*Foxp3*-Cre mice (magnification: left, ×4; scale 1mm and right, ×20; scale 200 μm). Data are representative of at least two independent experiments (**a-f**). *$P < 0.05$ and **$P < 0.001$. Data are mean ± s.e.m.

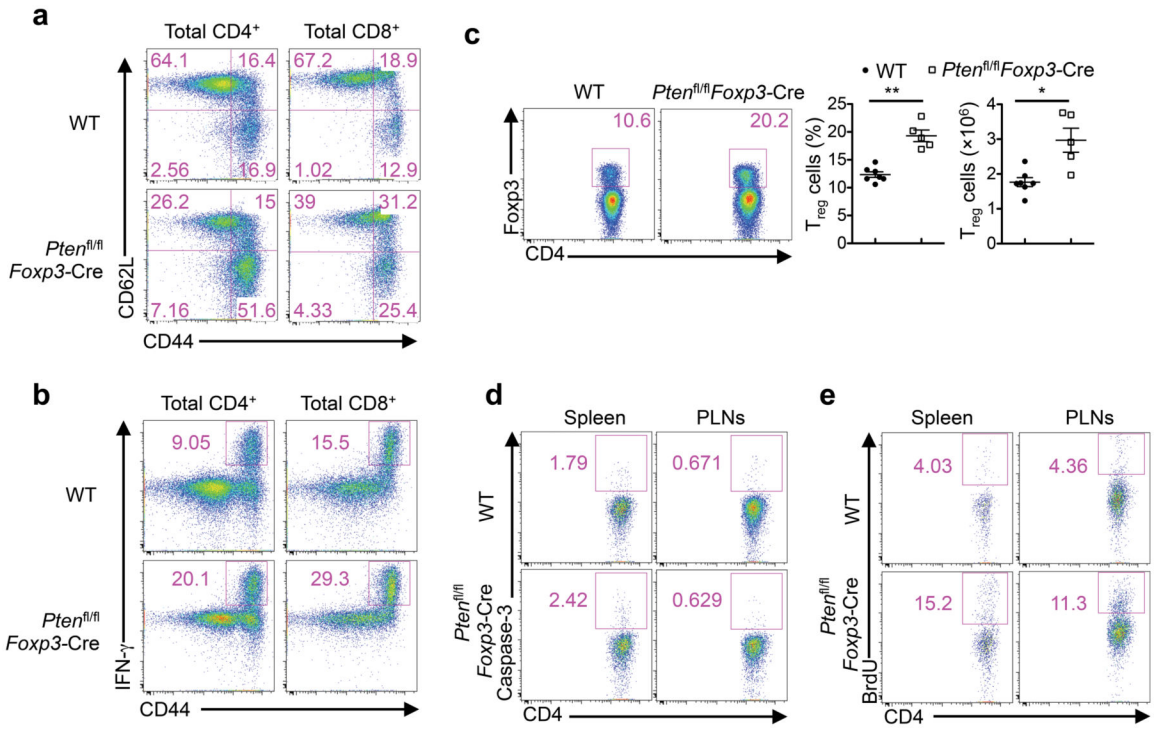

Figure 2. Increased T cell activation and altered immune homeostasis in *Pten*$^{fl/fl}$*Foxp3*-Cre mice

(**a**) Expression of CD62L and CD44 on WT and *Pten*$^{fl/fl}$*Foxp3*-Cre splenic T cells. Numbers in quadrants indicate percent cells in each. (**b**) Expression of IFN-γ in CD4$^+$ and CD8$^+$ T cells of WT and *Pten*$^{fl/fl}$*Foxp3*-Cre mice. (**c**) Flow cytometry analysis of T_{reg} cells in WT and *Pten*$^{fl/fl}$*Foxp3*-Cre splenic CD4$^+$ T cells. Below, the frequency and numbers of T_{reg} cells. (**d,e**) Caspase-3 activity (**d**) and BrdU staining at 16 h after injection of BrdU (**e**) in T_{reg} cells from the spleen and peripheral lymph nodes (MLNs) of WT and *Pten*$^{fl/fl}$*Foxp3*-Cre mice. Data are representative of at least ten independent experiments (**a-c**) and two independent experiments (**d,e**). **P* < 0.05 and ***P* < 0.001. Data are mean ± s.e.m.

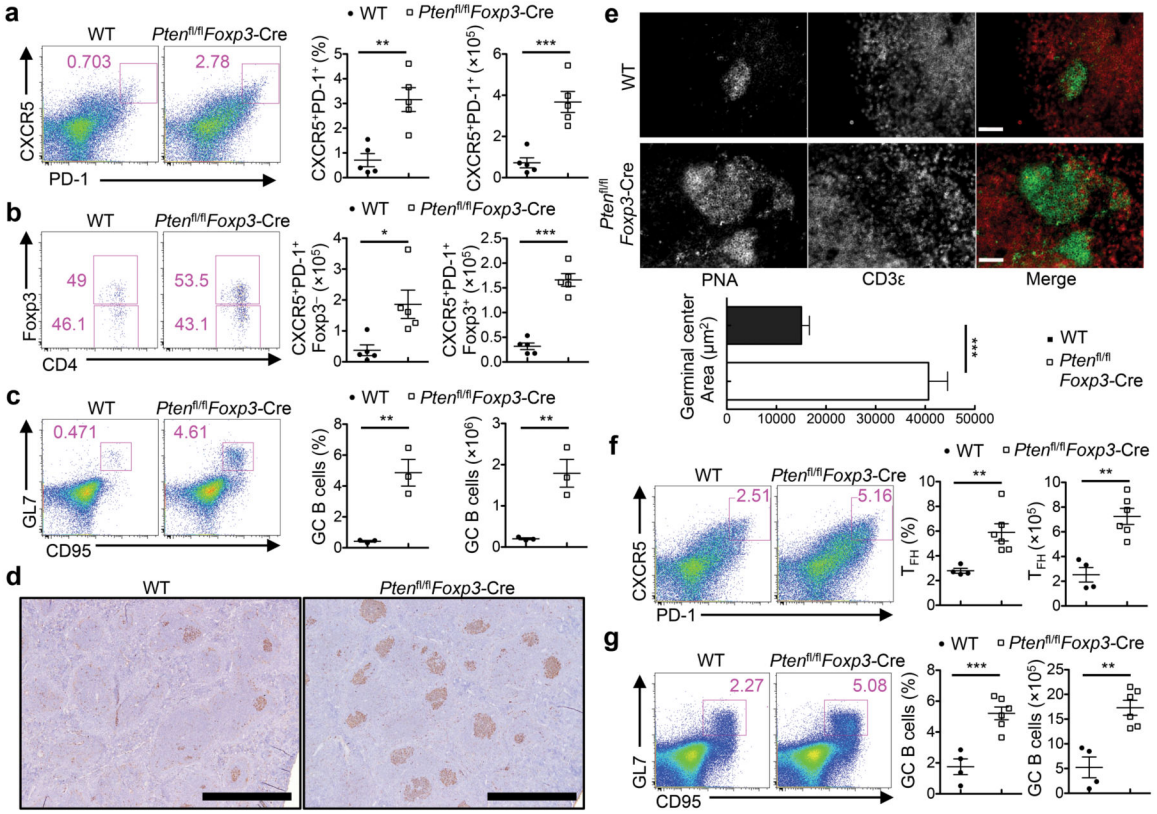

Figure 3. The aberrant induction of T_{FH} cell and GC responses in *Pten*$^{fl/fl}$*Foxp3*-Cremice

(**a**) Flow cytometry analysis of CXCR5$^+$PD-1$^+$ cells (gated on CD4$^+$TCRβ$^+$ cells) in the spleen of WT and *Pten*$^{fl/fl}$*Foxp3*-Cremice. Right, the frequency and numbers of T_{FH} cells. (**b**) Analysis of conventional T_{FH} (CD4$^+$CXCR5$^+$PD-1$^+$Foxp3-YFP$^-$) and T_{FR} cells (CD4$^+$CXCR5$^+$PD-1$^+$Foxp3-YFP$^+$) in the spleen of WT and *Pten*$^{fl/fl}$*Foxp3*-Cremice. (**c**) Analysis of GL7$^+$CD95$^+$ GC B cells (gated on CD19$^+$ B cells) in the spleen of WT and *Pten*$^{fl/fl}$*Foxp3*-Cremice. Right, the frequency and numbers of GC B cells. (**d**) PNA staining of spleen sections of WT and *Pten*$^{fl/fl}$*Foxp3*-Cremice (magnification, ×4; scale 1mm). (**e**) Immune fluorescence of MAN sections of WT and *Pten*$^{fl/fl}$*Foxp3*-Cremice for the staining of CD3 (red) and PNA (green) (scale 60 μm). Bottom, quantification of germinal center area. (**f,g**) Analysis of T_{FH} (**f**) and GC B cells (**g**) in the spleen of mice immunized with SRBCs 7 days previously. Data are representative of at least ten independent experiments (**a-c**) and two independent experiments (**d-g**). *P < 0.05, **P < 0.01 and ***P < 0.001. Data are mean ± s.e.m.

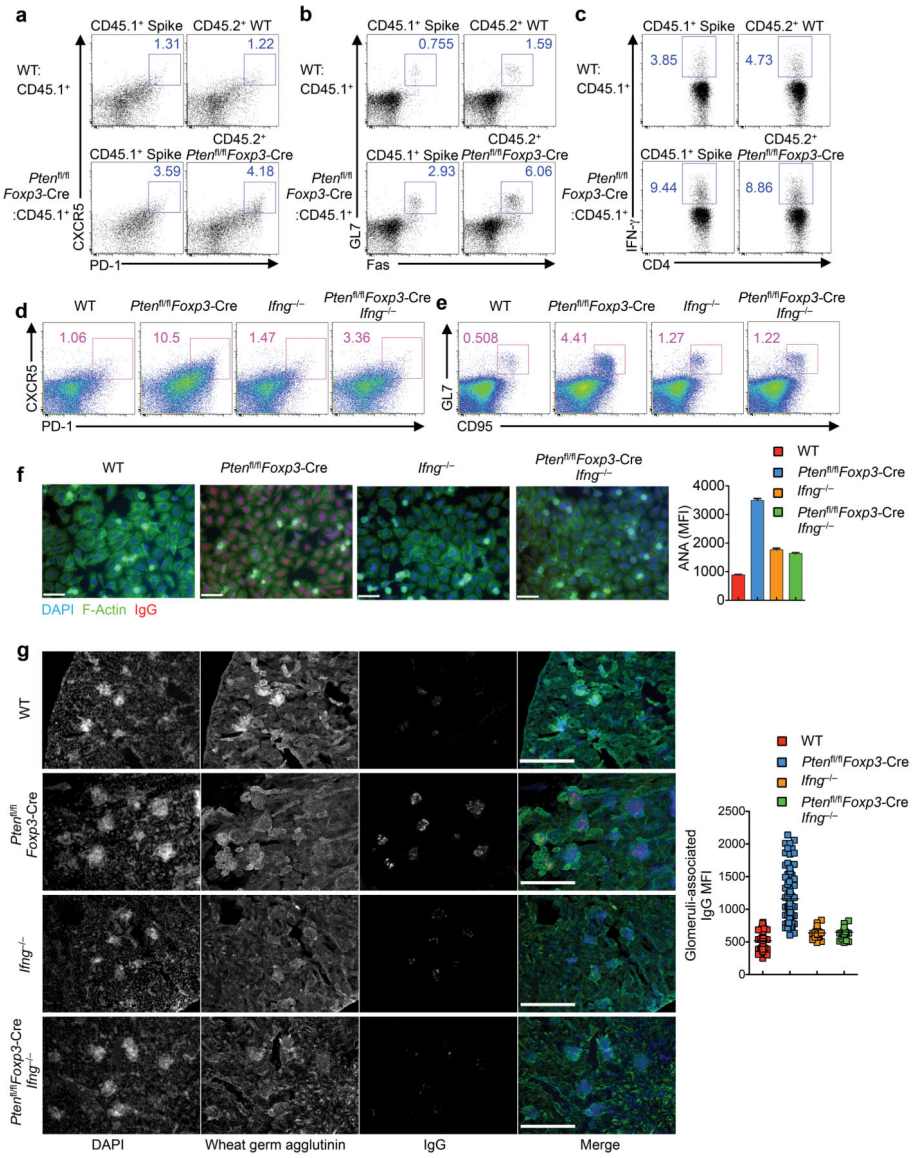

Figure 4. Analysis of bone marrow-derived chimeras and *Pten*$^{fl/fl}$*Foxp3*-Cre *Ifng*$^{-/-}$ mice reveals an important contribution of IFN-γ overproduction to dysregulated T_{FH} responses in *Pten*$^{fl/fl}$*Foxp3-Cre* mice

(**a-c**) Sublethally irradiated *Rag1*$^{-/-}$ mice were reconstituted with a 1:1 mix of CD45.1^{+} BM and either CD45.2^{+} WT or *Pten*$^{fl/fl}$*Foxp3*-Cre BM cells. Following reconstitution, the mixed chimeras were analyzed for T_{FH} (**a**), GC B cells (**b**), and intracellular staining of IFN-γ in CD4^{+} T cells (c). (**d,e**) Analysis of T_{FH} (**d**) and GC B cells (**e**) in the spleen of WT, *Pten*$^{fl/fl}$*Foxp3*-Cre, *Ifng*$^{-/-}$ and *Pten*$^{fl/fl}$*Foxp3*-Cre *Ifng*$^{-/-}$ mice. (**f**) Representative images and quantification of fluorescent intensity (right) of ANA IgG autoantibodies detected with Hep-2 slides in the serum from WT, *Pten*$^{fl/fl}$*Foxp3*-Cre, *Ifng*$^{-/-}$ and *Pten*$^{fl/fl}$*Foxp3*-Cre *Ifng*$^{-/-}$ mice (scale 60 μm). (**g**) Representative images of immune fluorescence imaging of kidney sections showing IgG deposits (scale 300 μm), and quantitative analysis (right). Data are representative of three independent experiments (**a-e**) and one experiment (**f,g;** n=3 WT,

6 *Pten*$^{fl/fl}$*Foxp3*-Cre, 2 *Ifng*$^{-/-}$ and 3 *Pten*$^{fl/fl}$*Foxp3*-Cre *Ifng*$^{-/-}$ mice). Data are mean ± s.e.m.

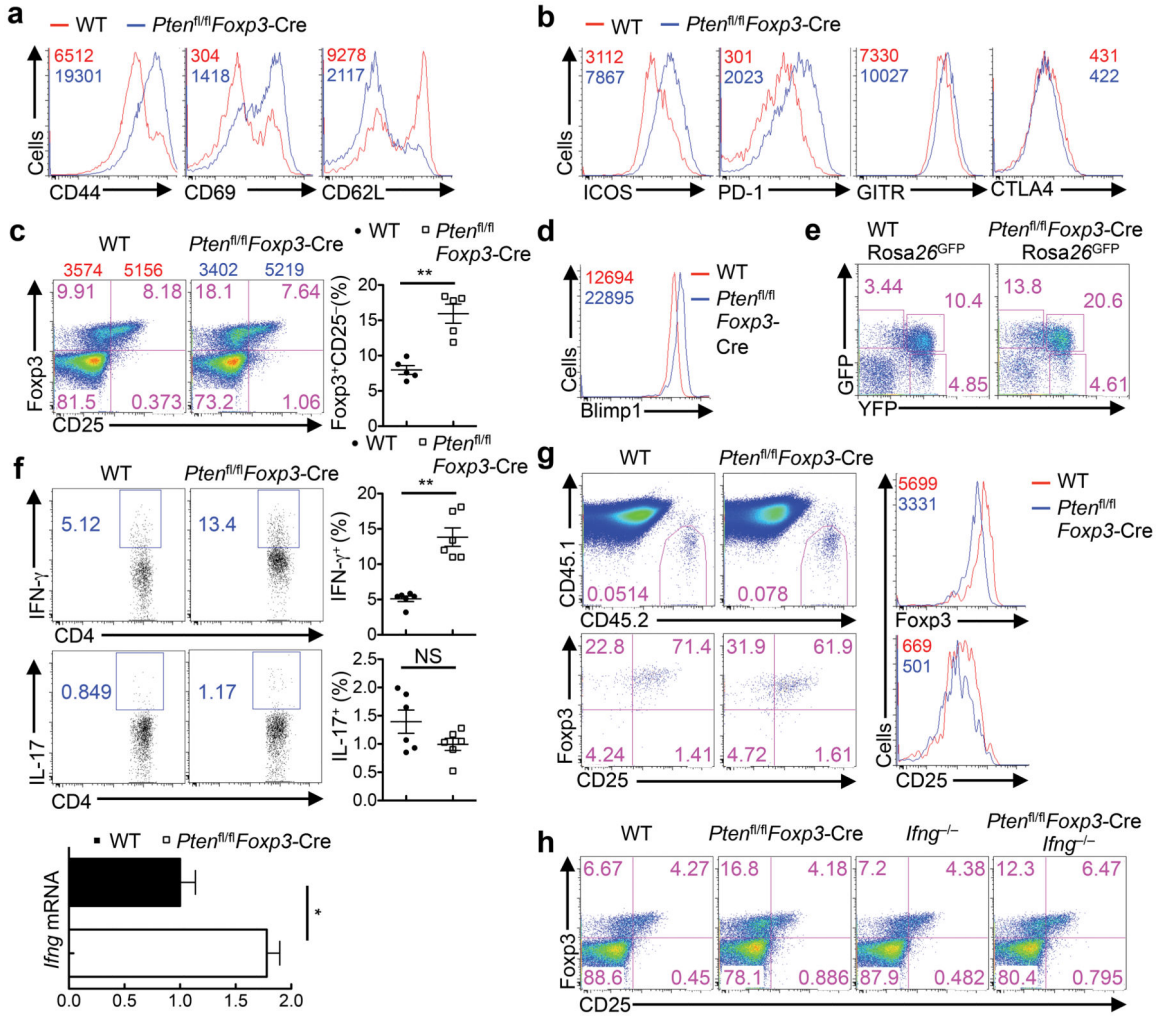

Figure 5. PTEN deficiency impairs T_{reg} stability

(**a,b**) Expression of CD44, CD69, CD62L (**a**) and ICOS, PD-1, GITR and CTLA4 (**b**) in T_{reg} cells from the spleen of WT and *Pten*$^{fl/fl}$*Foxp3*-Cre mice. Mean fluorescent intensity (MUFI) is presented in the plots. (**c**) Expression of CD25 and Foxp3 (gated on CD4$^+$TCRβ$^+$ cells) in the spleen of WT and *Pten*$^{fl/fl}$*Foxp3*-Cremice; the numbers above the graphs indicate the mean fluorescent intensity (MUFI) of Foxp3 in CD25$^-$ and CD25$^+$ subsets. Right, quantification of Foxp3$^+$CD25$^-$ cells. (**d**) Expression of Blimp1 in the splenic T_{reg} cells of WT and *Pten*$^{fl/fl}$*Foxp3*-Cre mice. (**e**) Foxp3-YFP and GFP expression in CD4$^+$ T cells from *Pten*$^{+/+}$*Foxp3*-Cre Rosa26^{GFP}and *Pten*$^{fl/fl}$*Foxp3*-Cre Rosa26^{GFP}mice. (**f**) Intracellular staining of IFN-γ and IL-17 (right, quantification of IFN-γ$^+$ and IL-17$^+$ producing cells in T_{reg} cells), and RNA analysis of IFN-γ in T_{reg} cells of WT and *Pten*$^{fl/fl}$*Foxp3*-Cre mice (IL-17 RNA was undetectable). (**g**) WT and *Pten*$^{fl/fl}$*Foxp3*-Cre T_{reg} (CD45.2$^+$) were transferred into CD45.1$^+$ recipients, followed by analysis of donor cell percentages (upper) and Foxp3 and CD25 expression (lower). Right, direct overlays of donor-derived WT and *Pten*$^{fl/fl}$*Foxp3*-Cre T_{reg} cells for Foxp3 (upper right) and CD25 levels (lower right). (**h**) Flow cytometry analysis of Foxp3-YFP$^+$CD25$^-$ cells in WT, *Pten*$^{fl/fl}$*Foxp3*-Cre, *Ifng*$^{-/-}$ and *Pten*$^{fl/fl}$*Foxp3*-Cre *Ifng*$^{-/-}$ splenic T_{reg} cells. Data are

representative of at least three independent experiments (**a-f, h**) and two independent experiments (**g**). NS, not significant; *$P < 0.05$ and **$P < 0.001$. Data are mean ± s.e.m.

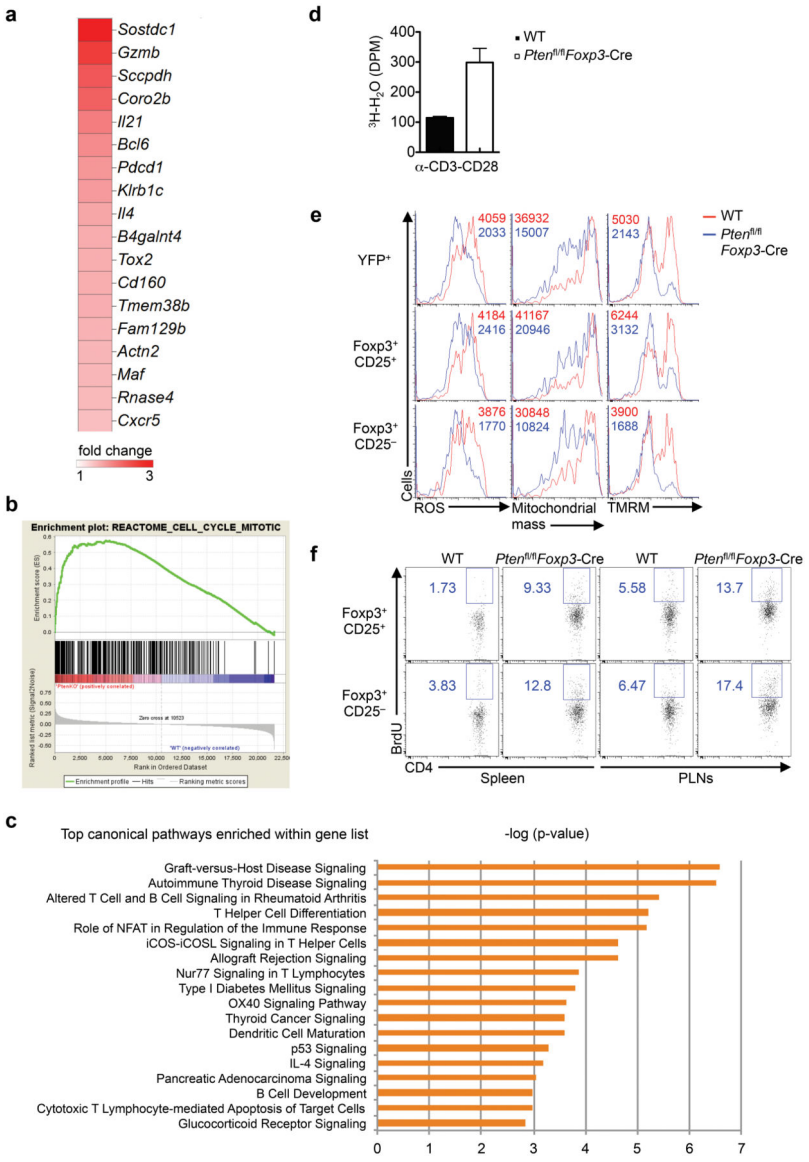

Figure 6. PTEN-dependent gene expression and metabolic programs in T_{reg} cells

(**a**) Heat maps display expression, relative to the WT mean (over or equivalent to 1.5 fold), of T_{FH}-related genes. (**b**) GSEA reveals the cell cycle mitotic pathway as one of the most extensively upregulated pathways in *Pten*$^{fl/fl}$*Foxp3*-Cre T_{reg} cells. (**c**) IPA analysis of canonical pathways controlled by PTEN in T_{reg} cells. (**d**) Glycolytic activity of T_{reg} cells stimulated with α-CD3-CD28. (**e**) Analysis of ROS production, mitochondrial mass and mitochondrial membrane potential (tetramethylrhodamine, methyl ester, TMRM) in T_{reg} cells of WT and *Pten*$^{fl/fl}$*Foxp3*-Cremice. (**f**) Analysis of BrdU incorporation in T_{reg} subsets of WT and *Pten*$^{fl/fl}$*Foxp3*-Cremice. Data are representative of one experiment (**a-c**; n=3 WT, 3 *Pten*$^{fl/fl}$*Foxp3*-Cre mice), two independent experiments (**d,f**) and three independent experiments (**e**).

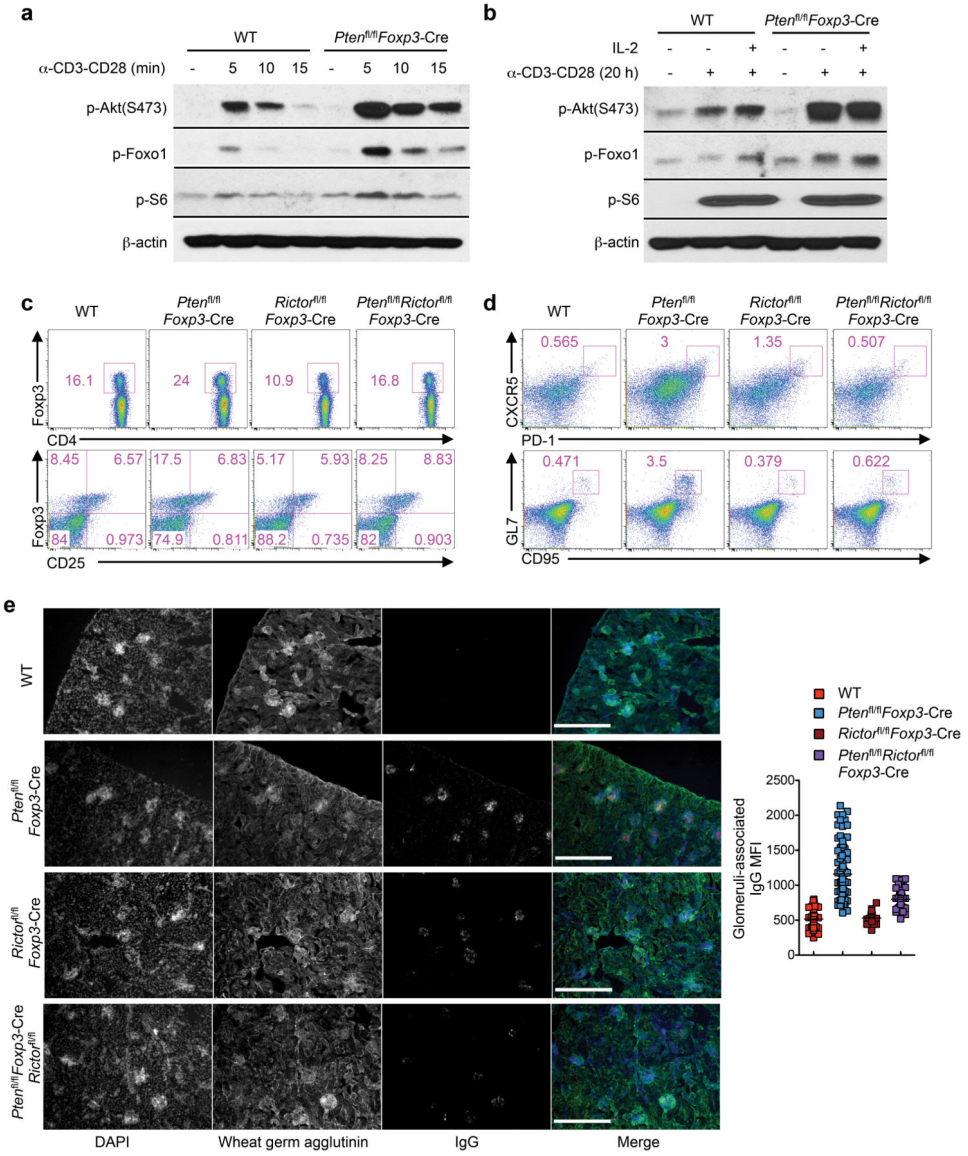

Figure 7. Dysregulated mTORC2 activity in PTEN-deficient T_{reg} cells responsible for the immune tolerance breakdown

(**a,b**) Immunoblots of phosphorylation of Akt (S473), Foxo1 and S6 in resting and short-term stimulated T_{reg} cells (**a**) and in resting and long-term stimulated T_{reg} cells (**b**) isolated from WT and *Pten*$^{fl/fl}$*Foxp3*-Cre mice. (**c,d**) Flow cytometry analysis of WT, *Pten*$^{fl/fl}$*Foxp3*-Cre, *Foxp3*^{cre}*Rictor*$^{fl/fl}$ and *Pten*$^{fl/fl}$*Rictor*$^{fl/fl}$*Foxp3*-Cremice for Foxp3 (upper) and CD25 (lower) expression in CD4^{+} T cells (**c**), and proportions of FH cells (upper) and GC B cells (lower) (**d**). (**e**) Kidney sections showing IgG deposits (scale 300 μm) and quantification (right; quantitative results of WT and *Pten*$^{fl/fl}$*Foxp3*-Cre mice in Fig. 4g are shown here for comparison). Data are representative of two independent experiments (**a,b**), three independent experiments (**c,d**) and one experiment (**e**; n=2 *Foxp3*^{cre}*Rictor*$^{fl/fl}$ and 3 *Pten*$^{fl/fl}$*Rictor*$^{fl/fl}$*Foxp3*-Cremice). Data are mean ± s.e.m.

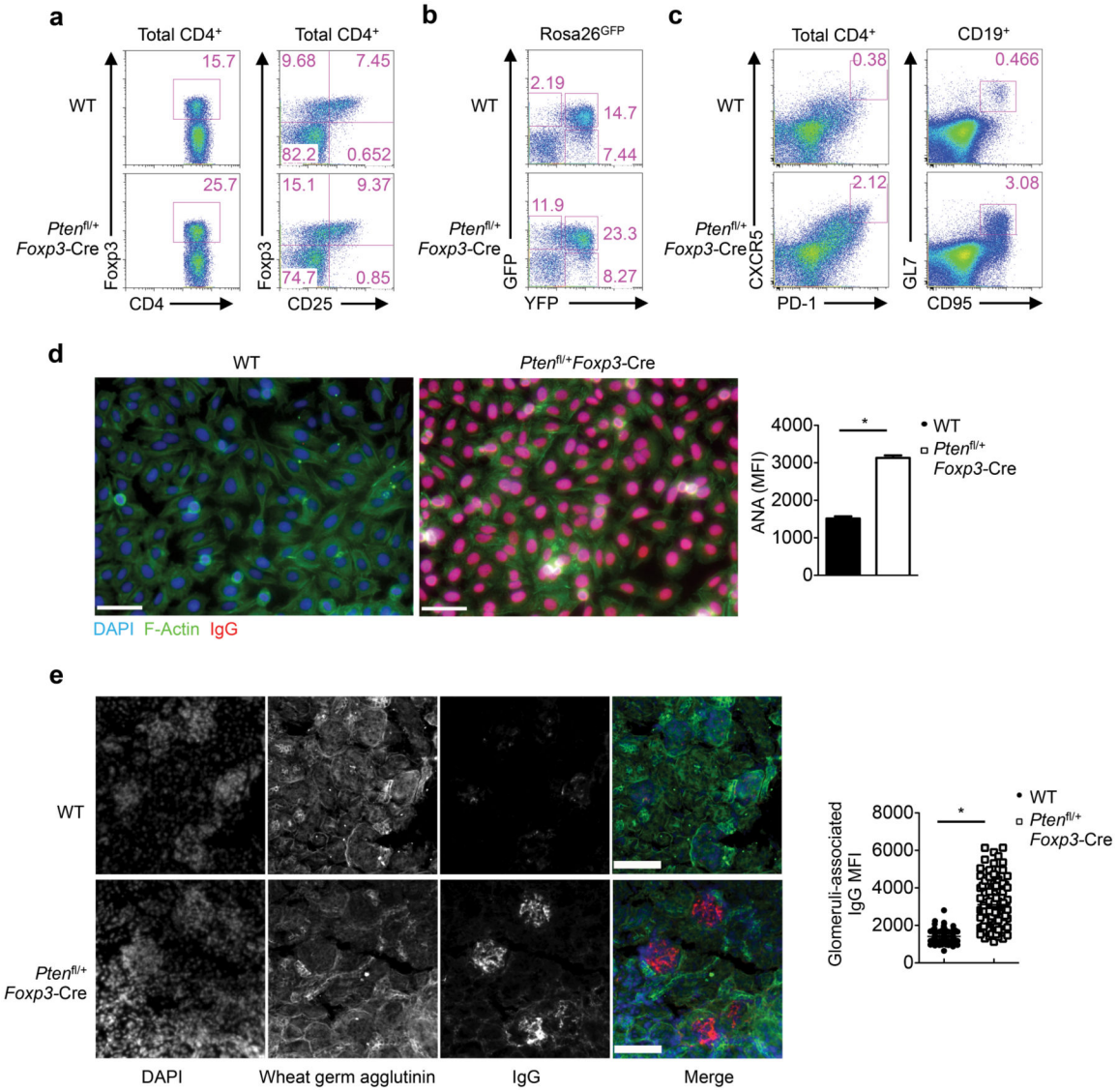

Figure 8. Heterozygous loss of PTEN in T_{reg} cells is sufficient to disrupt immune homeostasis

(**a**) Flow cytometry analysis of Foxp3 and CD25 expression in WT and *Pten*$^{fl/+}$*Foxp3*-Cresplenic CD4$^+$ T cells. (**b**) Foxp3-YFP and GFP expression in CD4$^+$ T cells from *Pten*$^{+/+}$*Foxp3*-CreRosa26^{GFP}and *Pten*$^{fl/+}$*Foxp3*-Cre Rosa26^{GFP}mice. (**c**) Analysis of CXCR5$^+$PD-1$^+$ cells (gated on CD4$^+$TCRβ$^+$ cells) and GL7$^+$CD95$^+$ GC B cells (gated on CD19$^+$ B cells) in the spleen of WT and *Pten*$^{fl/+}$*Foxp3*-Cre mice. (**d**) Representative images (scale 60 μm) and quantification of fluorescent intensity (right) of serum ANA IgG autoantibodies detected with fixed Hep-2 slides. (**e**) Immune fluorescence images of kidney glomeruli sections showing IgG deposits (scale 100 μm). Data are representative of at least two independent experiments (**a-e**). *P < 0.0001. Data are mean ± s.e.m.